

SUPPLEMENTAL MATERIAL

Chloroquine Terminates Stretch-Induced Atrial Fibrillation in the Sheep Heart More Effectively than Flecainide.

David Filgueiras-Rama, MD, Raphael Pedro Martins, MD, Sergey Mironov, PhD, Masatoshi Yamazaki, MD, Conrado Calvo, MSc, Steve R Ennis, PhD, Krishna Bandaru, MD, Sami F Noujaim PhD, Jérôme Kalifa, MD, Omer Berenfeld, PhD, José Jalife, MD.

Supplemental Methods.

Experimental Setup.

Stretch-induced atrial fibrillation in the Langendorff-perfused sheep heart.

The isolated, coronary perfused heart underwent an atrial trans-septal puncture to enable equalize intracavitary pressure in both atria. Tetrapolar electrode catheters (Torq®, Medtronic Inc./Minneapolis/MN/USA) were placed into each of the pulmonary veins (PVs) to record bipolar signals from the two distal electrodes (sampling rate, 1.0 kHz) using a Biopac Systems amplifier (DA100C; Biopac Systems, Inc., Goleta, CA, USA). Additional bipolar recordings were obtained from the top and roof of the left atrial appendage (LAA) and right atrial appendage (RAA). All vein orifices were then sealed, except the inferior vena cava, which was cannulated and connected to a digital sensor (Biopac Systems transducer-TSD104A; Biopac Systems, Inc., Goleta, CA, USA) and to an outflow cannula whose open-ended height above the atria controlled the intra-atrial pressure. The pressure was then

increased to 14 cm H₂O, which led to an increase in atrial volume and dilatation. The pressure was maintained stable throughout the experiment.¹

Epicardial mapping of the LAA and RAA.

A bolus injection of 5 to 10 ml Di-4-ANEPPS (10 mg/mL) (Sigma-Aldrich, St. Louis, MO, USA) and a loading period of 10 min are needed to obtain voltage-sensitive fluorescence upon laser excitation (532 nm) of the epicardial surface. The emitted fluorescence is then transmitted through a 600 nm long pass filter and projected onto LittleJoe CCD video camera (80x80 pixels, SciMeasure Analytical Systems, Inc. Decatur, GA, USA) and acquired at a rate between 500-1000 frames per second. Five-second movies were obtained at 2 min intervals during control AF. The area of the mapped epicardial surface was ~14 cm².

Endocardial optical mapping of the posterior left atrium (PLA) of the intact heart.

A second LittleJoe CCD camera (80x80 pixels) was synchronized with the epicardial camera. A 10 mm diameter dual-channel rigid borescope (Everest VIT, Inc. Flanders, NJ, USA) with a 90-degree field of view was introduced through the anterior wall of the left ventricle, across the mitral valve and focused on the endocardial surface of the PLA (supplemental Figure 1). The optically mapped area on the PLA was ~3.7 cm², which allowed visualizing the four PVs and the atrial septo-pulmonary bundle. The borescope was c-mounted to the CCD camera through a custom-made eyepiece adapter. Laser excitation (532 nm) was delivered to the endocardium through a liquid light-guide (0.2 in core).¹ In 7 experiments the endocardial surface of the PLA was optically mapped.

Experimental protocols.

As shown in Supplemental Figure 2A, the intra-atrial pressure was adjusted to 14 cm H₂O at the beginning of the protocol. Baseline pacing at 300, 250 and 200 ms was applied from the LAA. We used burst pacing at 12 Hz to induce AF, which was allowed to continue for a control period of 15 min, after which either chloroquine (N=7; 4 μM) or flecainide (N=5; 2-4 μM) was added to the Tyrode's solution. The drug concentration was doubled if AF persisted after 20 min under chloroquine or flecainide. A period of 50 min was allowed for AF termination to occur. AF was then terminated by DC shock (DFib) in those cases in which it persisted. AF re-induction was then attempted via burst pacing at 12 Hz, and was considered to be persistent when it lasted 15 min or longer after re-induction. Before washout a new DC shock (DFib) was used to restore the SR, if necessary. The washout period was 45 and 30 min for chloroquine and flecainide, respectively. Finally, after the washout, AF was re-induced by burst pacing and allowed to continue for 15 more min before the end of the protocol.

Supplemental Figure 2B illustrates the protocol of an additional set of optical mapping experiments (N=11) in which we determined the effects of chloroquine and flecainide on action potential duration and conduction velocity during pacing. Mapping and pacing were conducted on the epicardial surface of the LAA. The pacing protocol (300, 250 and 200 ms CL) was carried out at baseline, after 15 min of chloroquine (N=5) or flecainide (N=6), and after the washout. Representative electrograms are shown below the time-course of both protocols.

Atrial fibrillation dynamics.

Analysis of AF dynamics takes advantage of phase movies generated via Hilbert transformation.² Patterns of activation allow identifying rotors and breakthroughs.

• A rotor was identified by the presence of all phases converging on a singularity point (SP) lasting more than one rotation. Supplemental Figure 3A shows snapshots of the PLA after generation of phase maps: a rotor pattern is identified lasting for 3 rotations; from frame 0 to frame 114.

• A breakthrough was defined as a wavefront appearing in the field of view and propagating outward in a target-like pattern. Supplemental Figure 3B shows a breakthrough pattern in the PLA after generation of phase maps.

Quantification of the core size.

During functional reentry, the perimeter of the center of rotation (the “core”) is inscribed by the trajectory of the rotating SP that is formed after a wavebreak.³ As it completes full rotations, the SP in fact becomes the rotor that organizes the overall reentrant activity. The core size and shape reflect critical parameters of the excitable medium that control the frequency and dynamics of a stationary rotor responsible for generating spiral waves (SW). Typically during AF in the sheep left atrium, the cores of identifiable stationary rotors are ellipsoidal and have an area of $\sim 4 \text{ mm}^2$.⁴ However, most rotors that are observed during AF are non-stationary. In addition, particularly in the area with the highest frequency, multiple drifting rotors may form locally and then become extinct after highly variable lifetimes, which

makes it difficult to accurately quantify their properties. In addition, as they drift through the atrial muscle their cores no longer appear elliptical. Instead, their fingerprint in an amplitude map (see supplemental Figure 4)) is an extended dark band (i.e., a “line of block”) whose dimensions (width and length) depend on the velocity of impulse propagation, the speed of the core drift, and the lifespan of the individual rotor, and whose width provides an accurate measure of the core diameter. Here, we present a technique that allowed us to estimate the core widths of non-stationary rotors during control AF and during AF in the presence of chloroquine or flecainide (see Figure 5B and 6C in main manuscript). Our approach took advantage of the fact that during optical mapping of reentry the amplitude of the fluorescence signal at the core is appreciably lower than outside the core. Thus, as the rotor drifts into a camera pixel location, its core leaves a low fluorescence mark at that location. Supplemental Figures 4-6 illustrate this new method.

Supplemental Results

Supplemental Figure 7 shows the time-course of the DF_{\max} , number of rotations/cm² (PLA/LAA) and number of breakthroughs/cm² during control AF and after the administration of either chloroquine (Panel A) or flecainide (Panel B). Two representative cases are shown; one under chloroquine and one under flecainide. In panel A, the DF_{\max} sharply decreases after chloroquine, along with the number of rotations/cm² and breakthroughs/cm². Few number of identifiable rotations/cm² are present before AF termination under chloroquine (Figure 7A, central panel). In panel B, DF_{\max} slightly decreases after flecainide. The number

of identifiable rotations/cm² and breakthroughs/cm² also decrease, however the effect is not as strong as the chloroquine effect and the AF does not terminate.

Additional experiments (N=5) were performed at 1 μ M chloroquine. Such a concentration has less blocking effects on I_{Kr} (38%) and I_{Na} (14%), but I_{K1} is still highly blocked (74%).⁵ Supplemental Figure 8A shows how low doses of chloroquine (1 μ M) were able to terminate AF in 4 out of 5 AF episodes. In one AF episode chloroquine concentration was increased to 2 μ M to terminate the arrhythmia. In panel B, representative electrograms from the left superior PV (LSPV) show the restoration of SR under 1 μ M chloroquine. In panel C, control DF_{max} was similar in all chloroquine groups, with a significant decrease in DF_{max} before restoration of SR. The DF_{max} decreased from 10.6 ± 0.7 to 6.3 ± 0.2 Hz in the first few minutes after 4 μ M chloroquine, and from 10.5 ± 0.8 Hz to 6.7 ± 0.2 Hz after 1-2 μ M chloroquine and before the resumption of the SR.

Supplemental References.

1. Filgueiras-Rama D, Martins RP, Ennis SR, Mironov S, Jiang J, Yamazaki M, Kalifa J, Jalife J, Berenfeld O. High-resolution endocardial and epicardial optical mapping in a sheep model of stretch-induced atrial fibrillation. *J Vis Exp*. 2011:e3103.
2. Warren M, Guha PK, Berenfeld O, Zaitsev A, Anumonwo JM, Dhamoon AS, Bagwe S, Taffet SM, Jalife J. Blockade of the inward rectifying potassium current terminates ventricular fibrillation in the guinea pig heart. *J Cardiovasc Electrophysiol*. 2003;14:621-631.
3. Jalife J, Berenfeld O. Molecular mechanisms and global dynamics of fibrillation: An integrative approach to the underlying basis of vortex-like reentry. *J Theor Biol*. 2004;230:475-487.
4. Mandapati R, Skanes A, Chen J, Berenfeld O, Jalife J. Stable microreentrant sources as a mechanism of atrial fibrillation in the isolated sheep heart. *Circulation*. 2000;101:194-199.
5. Sanchez-Chapula JA, Salinas-Stefanon E, Torres-Jacome J, Benavides-Haro DE, Navarro-Polanco RA. Blockade of currents by the antimalarial drug chloroquine in feline ventricular myocytes. *J Pharmacol Exp Ther*. 2001;297:437-445.

Supplemental Figure legends.

Figure 1. Diagrammatic representation of the experimental setup used to map optically and electrically from the endocardial and epicardial surfaces of the left atrium. Epicardial bipolar electrograms were obtained from the PVs in all experiments.

Figure 2. Time-course of the experimental protocols. **A**, protocol to study AF termination after flecainide and chloroquine. **B**, protocol to study the effects of chloroquine and flecainide on action potential duration and conduction velocity during pacing. AF: atrial fibrillation. CL: cycle length. DFib: Defibrillation. SR: sinus rhythm.

Figure 3. **A**, snapshots of the PLA after generation of phase maps: a rotor pattern is identified lasting for 3 rotations; from frame 0 to frame 114. **B**, a breakthrough pattern in the PLA; Wavefront appearing in the field of view and propagating outward in a target-like pattern.

Figure 4. Panel **A** shows a single CCD camera pixel recording to illustrate the first step needed to build the amplitude maps used to measure core width. The peak fluorescence recorded by each pixel during each excitation (black) is counted as a fluorescence step (red) whose magnitude is measured from the zero fluorescence line, after correction of the baseline shift (blue). Panel **B** shows representative sequential amplitude maps obtained by the 80x80 pixel camera during propagation of a fibrillatory wavefront around a line of block. The frame time is indicated on the upper right corner of each frame. At time 0, the wavefront started from the top right corner of the field of view (red star), with the red arrows showing the wavefront location. Between frames 0 and 64, the same wavefront circumnavigated the line

of block, almost completing a full rotation before the next wave appeared at frame 95 (blue arrows).

Figure 5. The figure was taken from the same AF episode as figure 4. Panel **A** shows on the right a set of single pixel recordings for 4 sequential excitations recorded along the vertical red line on the amplitude map of panel **B**. In **A**, the upper recordings marked in red correspond to a wavefront that moved downward and from left to right during frames 150-250 in the map; the lower recordings are marked blue. On the left of panel A is the consolidated 3D amplitude profile across the dark band for the blue signals at frames 150 and the red signals at frame 200. Note that in each case the amplitude of the recordings gradually decreased toward the center of the map forming a clearly visible dark band. This dark band closely associated with singularity points (SPs). In panel **C** the red spots represent all the SPs obtained during propagation of the red wave. All the SPs were located inside the dark band, which clearly demonstrates that such a band is the fingerprint of a drifting core.

Figure 6. A and B, to measure the width of a dark band (panel **A**) we first draw an isoamplitude line (IAL) at about 30% of the maximal wave amplitude (panel **B**) to mark the dark band perimeter. Then lines are drawn perpendicular to the IAL across the width of the dark band at each relevant pixel location. The length of each perpendicular is a measure of the local core width. **C and D,** lines that do not encounter an IAL on both sides of the dark band are automatically excluded (green in panel C), as are lines whose angle was significantly different from 90 degrees (blue in panels C and expanded inset in D). In panel **E,** the obtained local core band width is plotted versus the distance along the IAL, where point 0 corresponds to the tip of the band (circle on panel B) and the shape of the plot is relatively

symmetrical at either side of point 0. Thereafter, all the obtained values for any particular band are averaged and the result is considered to be the width of that particular core.

Figure 7. Two representative cases are shown. **A**, the DF_{max} sharply decreases after chloroquine, along with the number of rotations/cm² and breakthroughs/cm². **B**, DF_{max} , the number of identifiable rotations/cm² and breakthroughs/cm² slightly decrease after flecainide (5-sec long movies were analyzed).

Figure 8. **A**, low doses of chloroquine (1 μ M) were able to terminate AF in 4 out of 5 AF episodes. **B**, representative electrograms from the left superior PV (LSPV) show the restoration of SR under 1 μ M chloroquine. **C**, control DF_{max} was similar in all chloroquine groups, with a significant decrease in DF_{max} before restoration of SR.

Figure 9. A, B, single pixel action potential from the LAA at baseline stretch (black), after chloroquine 4 μ M (red) and flecainide 4 μ M (blue). APD_{70} significantly prolongs after chloroquine. Conversely, non-significant changes are present after flecainide.

Supplemental Movie legends.

Movie 1. Phase movie showing a long meandering rotor anchored to the roof/PLA-LAA junction after 40 min of flecainide.

Movie 2. Phase movie of the posterior left atrium; short-lasting rotors (1-2 rotations) are present in control AF (chloroquine protocol).

Movie 3. Same AF episode as in Movie 2 after chloroquine; very few rotors are identified during the last minute before AF termination.

Movie 4. Phase movie of the posterior left atrium during control AF (flecainide protocol).

Movie 5. Same AF episode as in Movie 4; although reentrant activity decreases still persists after 50 min under flecainide.

Supplemental Figures.

Figure 1.

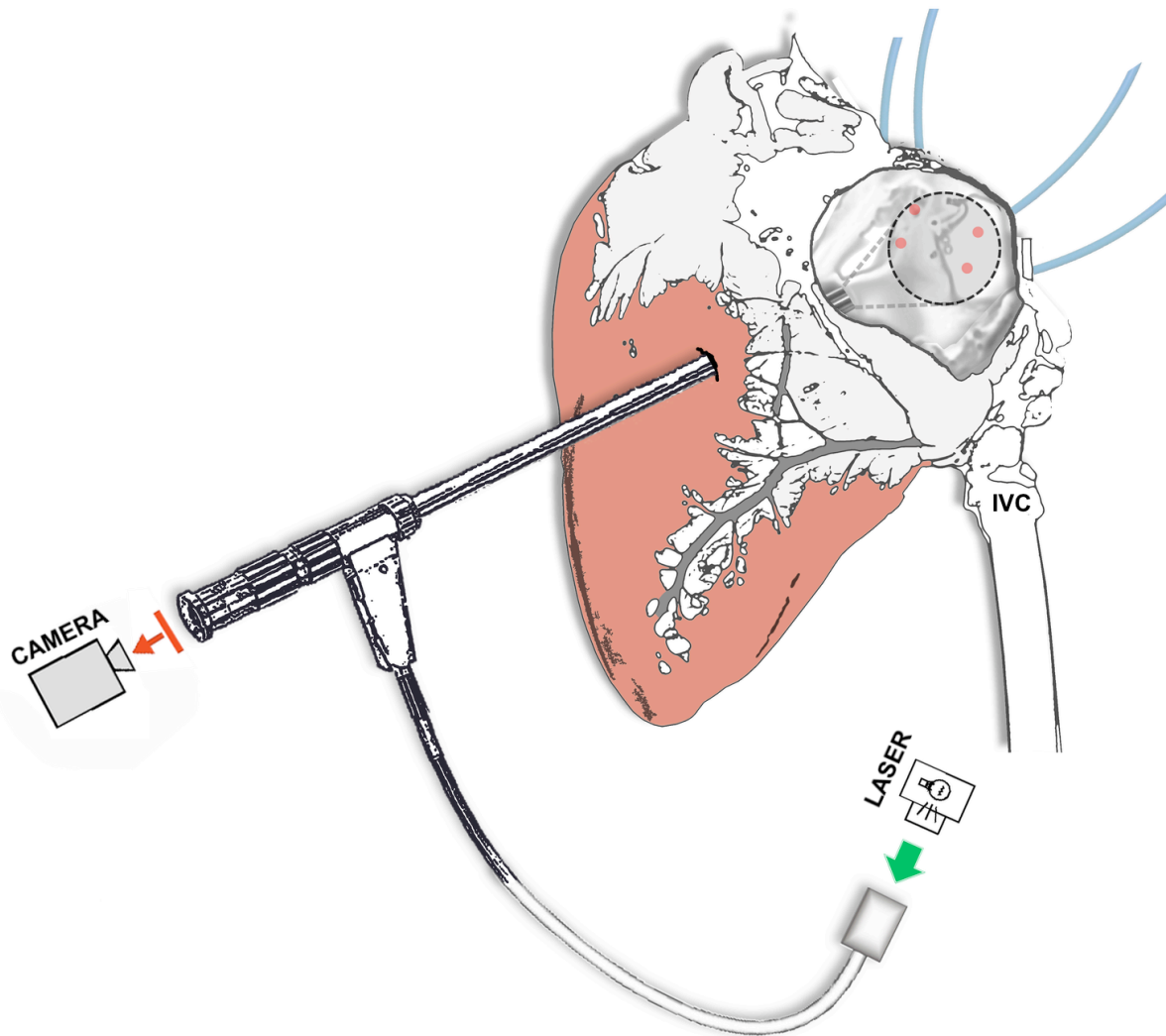


Figure 2.

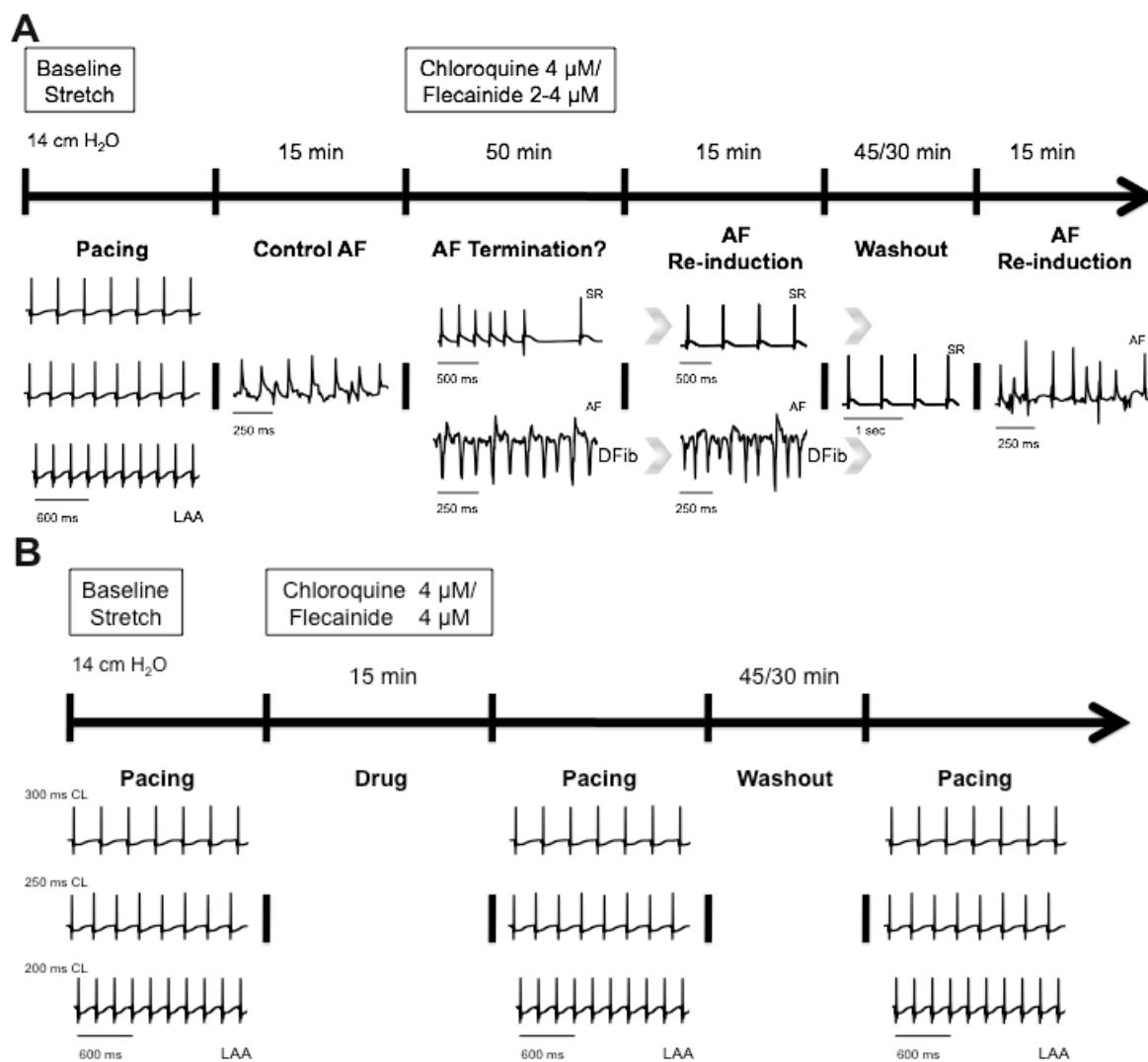


Figure 3.

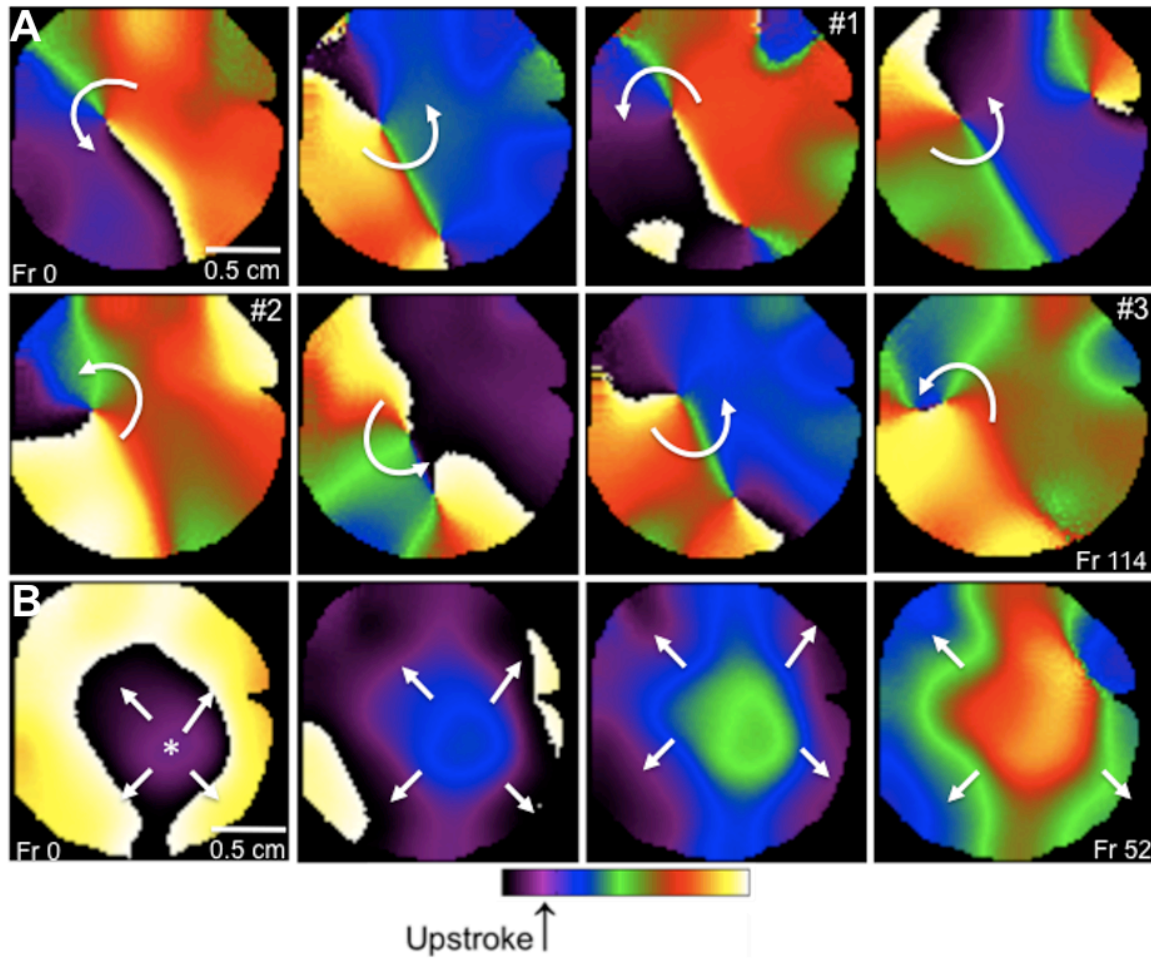


Figure 4.

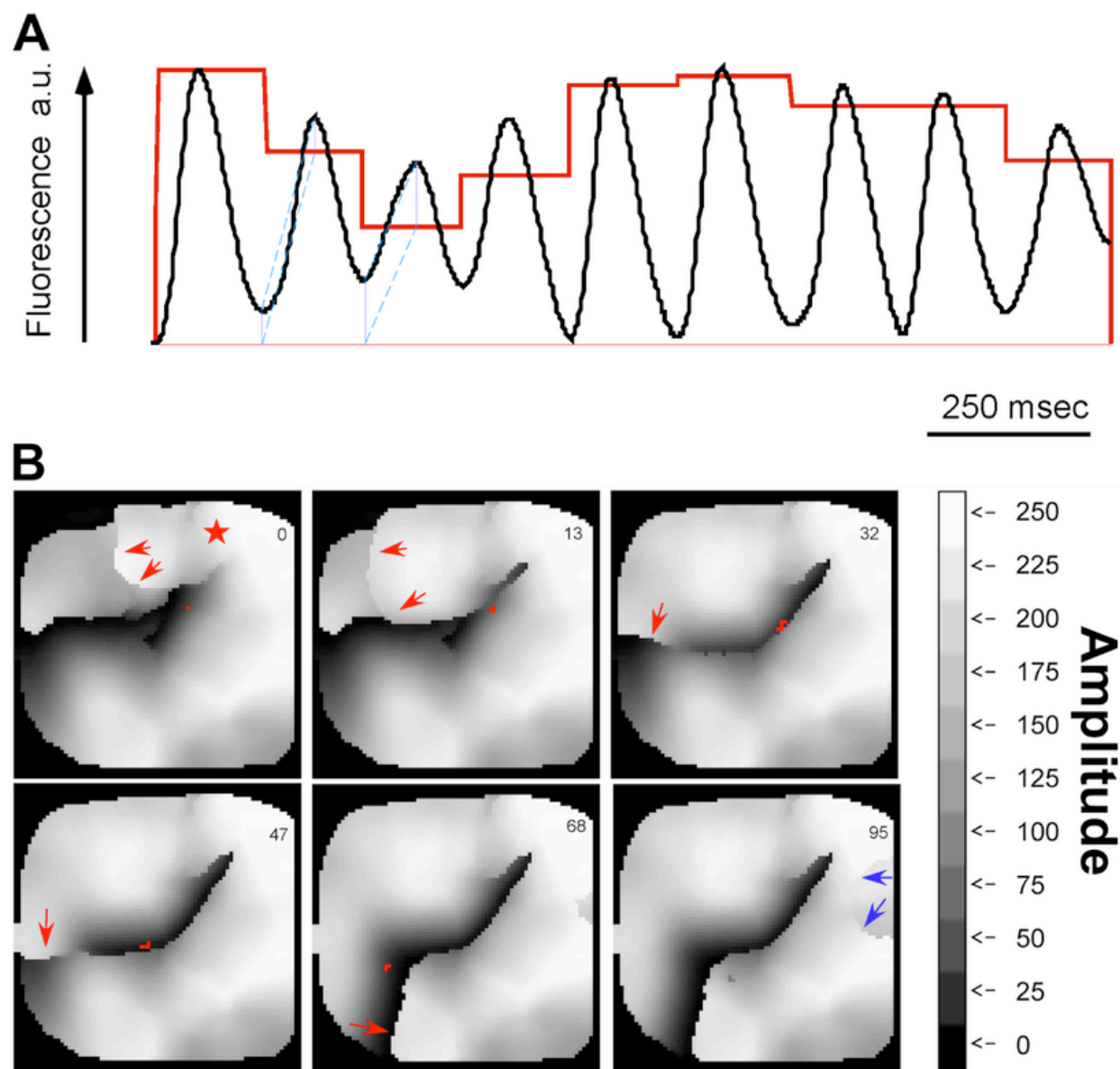


Figure 5.

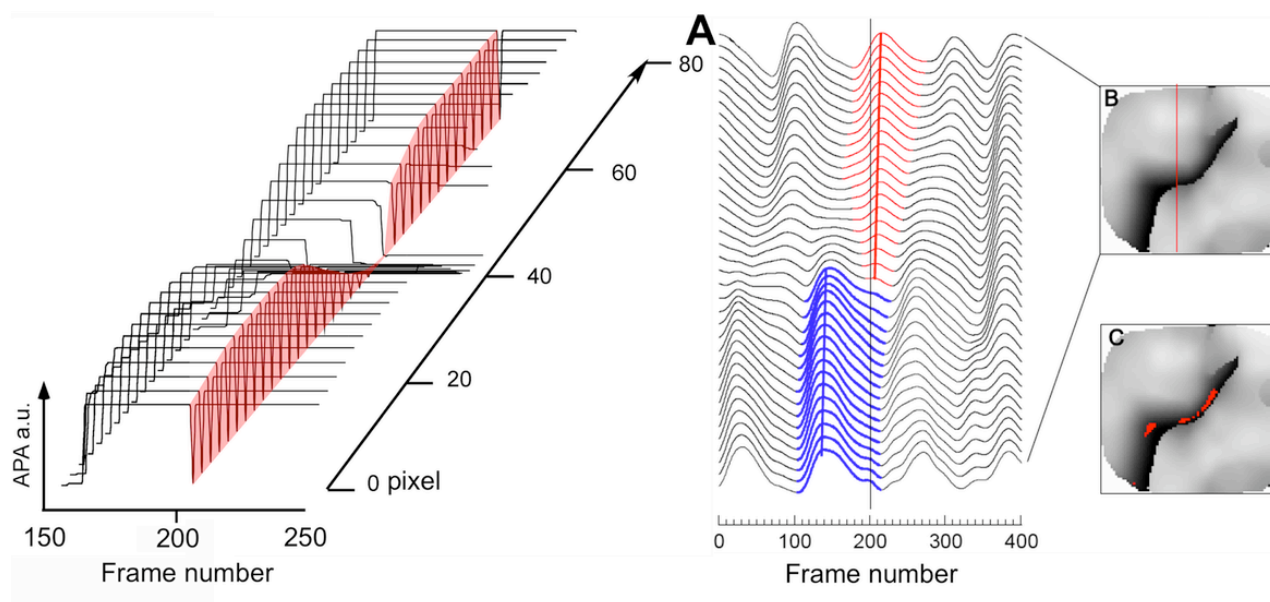


Figure 6.

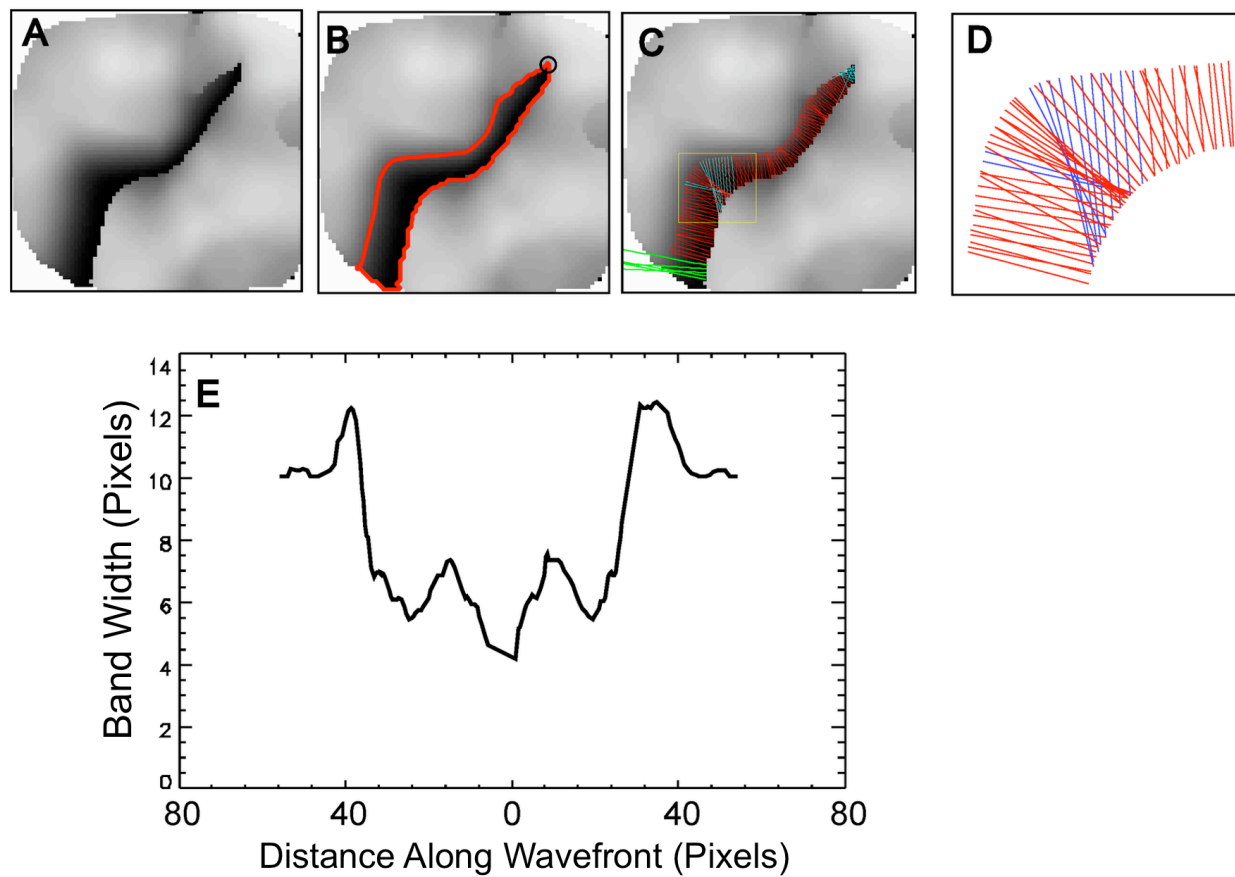


Figure 7.

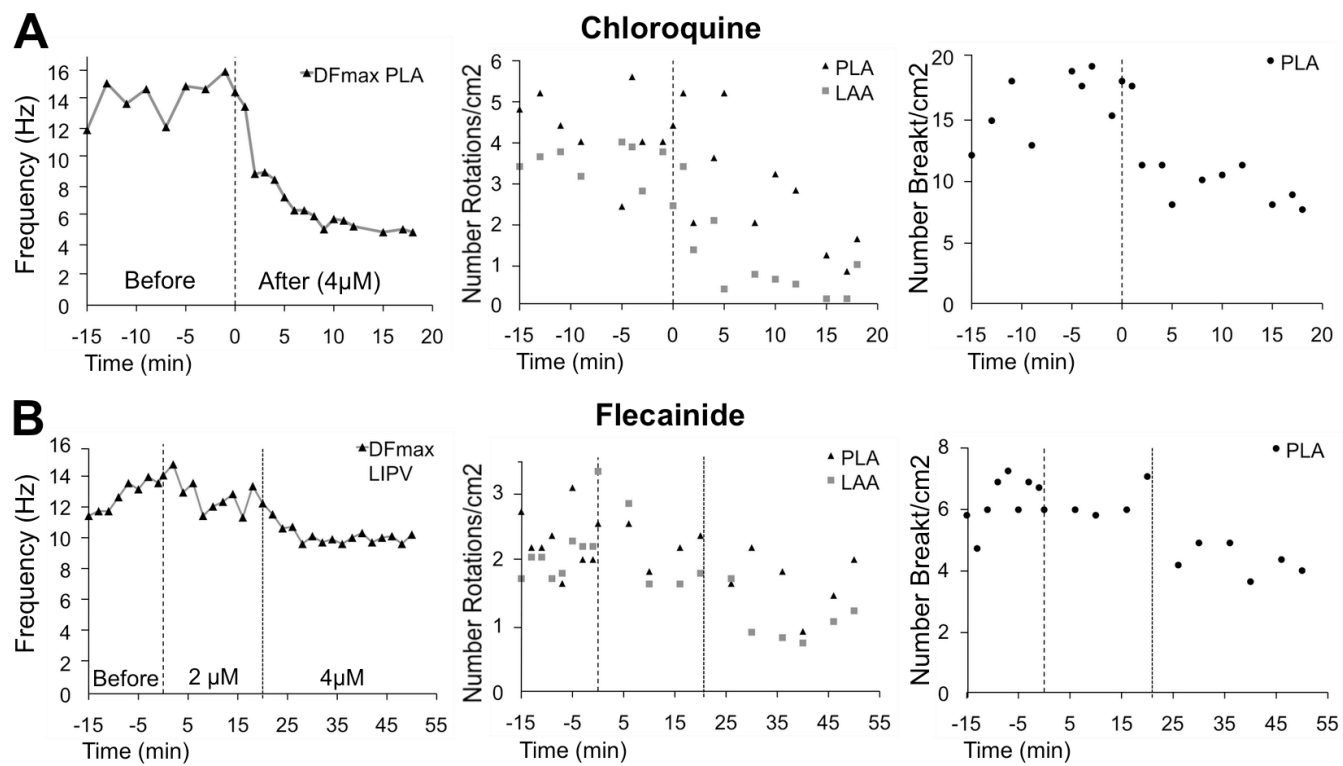


Figure 8.

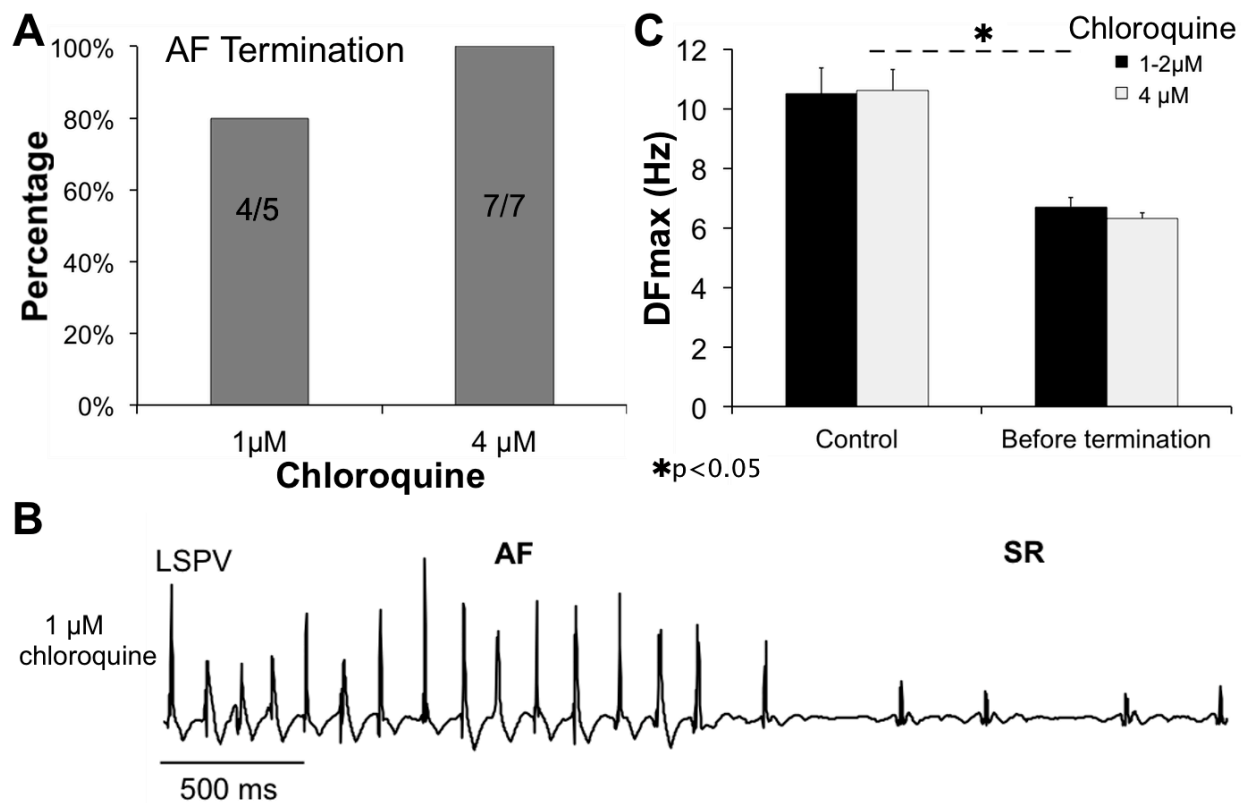


Figure 9.

